International Conference on HAZARDOUS WASTE : Sources, Effects and Management
12-16 December 1998, Cairo-Egypt

EG0000148

MC-5

Trace Analysis of Irradiated Granite Samples from Hiroshima by Laser Ablation Inductively Coupled Plasma Mass Spectrometry

M.A. Amr, A.I. Helal, N.F. Zahran,
J.S. Becker*, C. Pickhardt*, and H.-J. Dietze*

Nuclear Research Center, N.R.C., Atomic Energy Authority, Cairo13759, Egypt
**Centralabteilung für Chemische Analysen, Forschungszentrum Jülich GmbH, D-52425, Jülich, Germany*

ABSTRACT

Laser ablation inductively coupled plasma mass spectrometry (LA-ICP-MS) is widely accepted as a rapid and sensitive technique for trace elemental analysis of solid materials and for local analysis of inhomogeneous materials (such as geological samples). Due to its direct solid sample analysis capability, LA-ICP-MS (using a quadrupole-based ICP-MS and at the Research Center Jülich developed laser ablation system: Nd-YAG-laser, 226nm, 10Hz and 5 ns) is applied for the analysis of geological (granite) samples from Hiroshima. In order to prepare homogeneous targets, these samples were melted together with a lithium-borate mixture in a muffle furnace at 1050 °C. Furthermore, for investigating of matrix effects the powder of these samples is mixed with graphite and pressed as targets for laser ablation. The quantification of the analysis results was carried out using granite (GM) as standard reference material. The relative sensitivity coefficients (RSCs) for most elements, which were determined for correction of the measured values, varied between 0.3 and 3.

Key words: laser ablation / Inductively coupled plasma-mass spectrometry / Granite

INTRODUCTION

Laser ablation was developed as a special sample introduction system for solid samples into the ICP-MS. LA-ICP-MS is mostly applied with low cost and fast scanning mass spectrometers. The evaporation of the solid target material was carried out in a laser ablation chamber[1]. The evaporated and dissociated material (atoms, molecules, ablated particles) was transferred by transport gas (argon) in the inductively coupled plasma where the neutrals are dissociated and ionized. In contrast to LIMS, where evaporation and ionization occur simultaneously by a focused laser beam in a high vacuum chamber, both processes- the evaporation process of the solid samples material in the laser ablation camber and the post-ionization of neutrals in the inductively coupled plasma ion source- happen in LA-ICP-MS under normal pressure

and are separated in time and space[2]. An advantage of LA-ICP-MS compared to ICP-MS of aqueous solutions is not only the simple sample preparation but also the significant reduction in interferences of oxide ions, hydroxide ions and hydride ions with the analyte ions.

EXPERIMENTAL

The experimental setup of the LA-ICP-MS is shown in the Fig.(1). It consists of an arrangement for laser ablation and a commercial ICP-MS (Perken-Elmer SCIEX ELAN 6000, Germany). The equipment for laser ablation[3-5] comprises the laser, the optical arrangement for transferring the beam to the sample and the ablation cell containing the sample. The operating parameters for the Nd.:YAG laser and the ICP mass spectrometer are summarized in Table (1).

Table (1): the experimental conditions used in the measurements

Laser ablation conditions		ICP-MS conditions	
Wavelength	266 nm	Plasma power	1200 W
Pulse duration	5 ns	Dwell time	100 ms
Spot diameter	0.2 mm	Carrier gas flow	0.9 l/min Ar
Repetition frequency	10 Hz	Plasma gas flow rate	14 l/min Ar
Power density	10^{10} w/cm^2	Auxiliary gas flow rate	0.8 l/min Ar
Energy pulse	11 mJ		
Raster width	5mm x 5mm		

All of the optical components in the laser beam path, excluding the window through which the laser beam penetrates into the ablation cell, are anti-reflection-coated for 266 nm. This helps to suppress greatly reflection losses for this wavelength. The optical components and their arrangement are chosen in such away that they can cope with all wavelength ranging from the far UV to the near IR. For beam deflection a prism is therefore employed instead of a mirror. For the same reason, a beam splitter is used instead of dichroic mirror for monitoring the surface of the sample. In order to switch from one wavelength to another it is only necessary to install or remove the frequency multipliers and to change the dichroic mirrors inside the laser.

The ablation cell has been especially designed and constructed for this setup. It consists of an outer and an inner cylinder. The outer cylinder is made of BK7 glass and separates the surrounding air from the argon transport gas flow through the cell. The window through which the laser beam penetrates into the ablation cell is simply sealed by a vacuum grease. The inner quartz glass cylinder should prevent memory effects. The window and the inner cylinder can be changed very easily as required. The ablation cell is mounted on a computer-controlled transitional xyz-stage so as to position the sample.

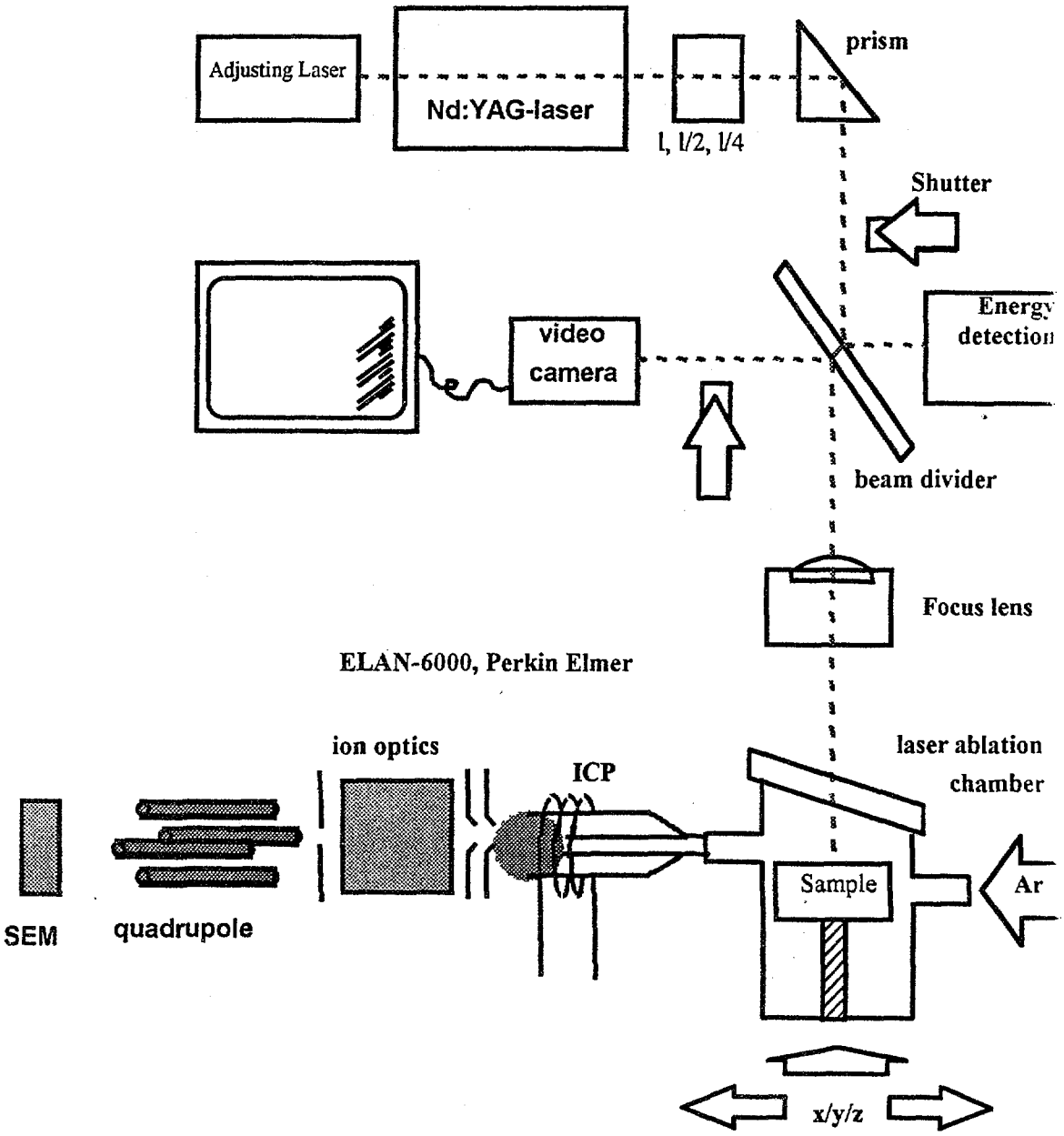

Fig. (1): schematic diagram of the laser ablation system coupled to the quadrupole mass spectrometer.

As the ablation rates vary non-linearly with the laser power, it is essential that the laser operates very stably. Unfortunately, it is very difficult to obtain a stable laser operation for λ = 266 nm with pulse energies of some tens of mJ. The best way to achieve stable laser operation is to turn the laser continuously for many hours and to select a particular laser pulse with the aid of shutter directly behind the laser. This is expected to enhance the reproducibility of the energy from pulse to pulse considerably. A second shutter in front of the video camera should protect it from too high intensities during the ablation process. The energy of the laser pulses during the ablation process is monitored with a laser energy meter (pyroelectric detector ED-200-SU from Gentech, Sainte-foy, Canada) by splitting the beam.

The laser, the two shutters, the transitional xyz-stage, the energy meter and the ICP-MS are synchronized and operated under computer control.

SAMPLE PREPARATION

Mass spectrometric methods allow the analysis of powdered or compact solid samples or layers directly without any expensive sample preparation. Two methods were used in order to prepare homogenizing targets of granite samples. A schematic diagram shown in Fig. (2) describes the steps of the method.

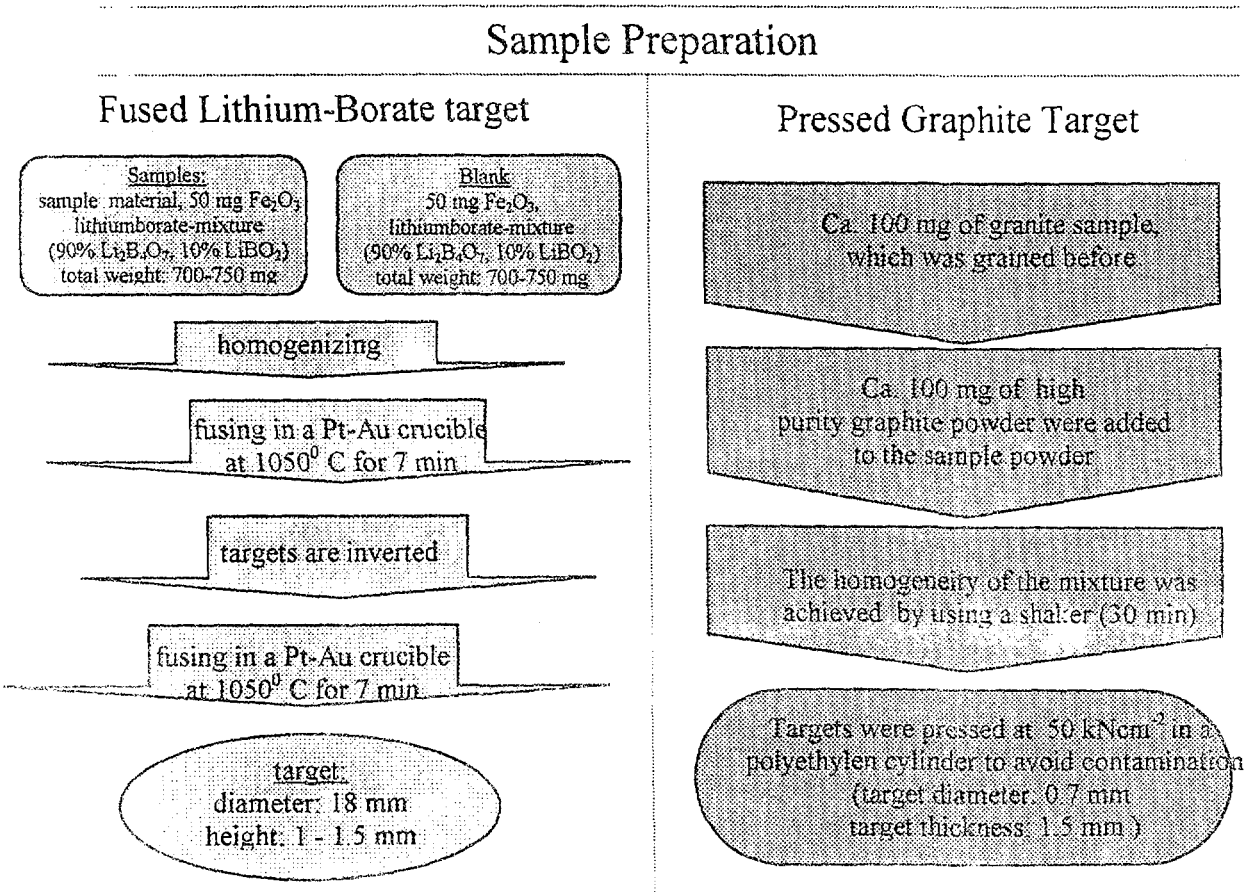

RESULTS AND DISSCASION

Limits of Detection

The determination of the limits of detection for solid-state analytical methods is always hampered a lack of suitable ultra high purity matrix-matched materials which can be used for the determination of the blank values. Therefore the gas blank[6] (intensities measured without laser shots) is sometimes used. Limits of detection obtained in this way certainly do not account for the increase of the background signals by the higher total number of ions increasing the pressure inside the mass spectrometer and the detector, for intensity increases by the peak shoulder of a neighboring matrix element or for interferences arising from molecules of matrix elements with argon, oxygen or nitrogen, double-charged ions, etc.. Becker et. al.[7] showed that the degree of metal argide ion formation (MAr^+/M^+) in ICP-MS was in the order of 10^{-7}–10^{-4}. This leads to a background interference up to several 1000 counts per second and thus to higher detection limits.

In this work we determined the detection limits ($LOD = \chi_B + 3x\sigma$, where χ_B is the mean value of background signal and σ the standard deviation) in matrix–matched blank samples were found to be lower. The limits of detection for impurities in granite GM in Lithium-borate and high purity graphite targets for LA-ICP-MS are summarized in table (2). Because of our determination procedure these values are on the safe side, as they can still be represented by real element concentrations. In case of Lithium-borate target the higher detection limit for Ni and Ag is due to iron oxide and contamination during sample preparation with Pt-Au crucibles, respectively. The higher detection limit for Cr , Ta and W are due to interference with $^{40}Ar^{12}C$ ion and contamination during sample preparation, because graphite target were pressed with Tantalum plat .

Quantification of analytical results

The quantification of results was carried out using granite GM as a standard reference material. The relative sensitivity coefficients (RSCs) were determined as shown in Fig. (3) to correct the measured values. RSCs are a function of the atomization energy and ionization potential of chemical elements and of the experimental parameters of mass spectrometric analysis. Correcting the measured concentrations of trace elements in granite GM with RSCs provides the accuracy of the analysis results with deviations of 10-20 %.

Trace Elements In Hiroshima Granite Samples

To establish general trends in trace-element results presented in tables (3) and (4) for Hiroshima Granite samples, the measured concentration of each element was compared with the reference values measured by different methods as explained in tables.

For sample 1, it was concluded that Sc, Cu, Ga, Nb, Mo, Sn, Gd, Tb, Dy, Ho, Er, Yb, Lu, Hf, Th and U showed accurate results with the reference values using high

Table (2): The detection limits (ppm) using granite (GM) standard reference material.

Analyzed Isotope	Graphite Target	Lithium Borate Target	Analyzed Isotope	Graphite Target	Lithium Borate Target
^{9}Be	0.94	8.04	^{140}Ce	0.02	0.19
^{45}Sc	0.26	1.05	^{141}Pr	0.003	0.04
^{51}V	0.27	19.16	^{142}Ce	0.02	0.23
^{52}Cr*	--	12.39	^{144}Nd	0.01	0.21
^{53}Cr	7.68	11.23	^{146}Nd	0.02	0.33
^{58}Ni (Fe)	0.05	3207.83#	^{147}Sm	0.02	0.33
^{59}Co	0.60	2.24	^{151}Eu	0.01	0.10
^{60}Ni	0.56	7.69	^{152}Sm	0.01	0.14
^{63}Cu	0.35	3.52	^{153}Eu	0.01	0.07
^{64}Zn	2.15	13.18	^{157}Gd	0.02	0.42
^{65}Cu	0.28	4.17	^{158}Gd	0.01	0.35
^{66}Zn	2.58	23.64	^{159}Tb	0.002	0.05
^{69}Ga	0.10	2.86	^{163}Dy	0.01	0.27
^{71}Ga	0.07	1.17	^{164}Dy	0.01	0.19
^{72}Ge	0.05	1.53	^{165}Ho	--	0.05
^{74}Ge	0.04	0.38	^{166}Er	0.01	0.10
^{75}As	0.05	2.01	^{167}Er	0.01	0.14
^{85}Rb	0.13	0.30	^{172}Yb	0.01	0.16
^{88}Sr	0.44	1.20	^{174}Yb	0.01	0.13
^{89}Y	0.02	0.10	^{175}Lu	0.002	0.03
^{90}Zr	0.83	0.95	^{178}Hf	0.02	0.15
^{93}Nb	0.02	0.16	^{180}Hf	0.01	0.10
^{94}Zr	0.85	1.25	^{181}Ta***	--	0.05
^{95}Mo	0.25	1.32	^{182}W***	--	0.86
^{98}Mo	0.39	1.46	^{184}W***	--	1.11
^{107}Ag**	0.02	--	^{200}Hg	0.05	0.59
^{109}Ag**	0.01	--	^{202}Hg	0.05	0.33
^{118}Sn	2.13	1.30	^{206}Pb	0.03	1.37
^{120}Sn	2.13	1.37	^{208}Pb	0.04	1.26
^{121}Sb	0.01	0.74	^{232}Th	0.002	0.16
^{123}Sb	0.01	1.04	^{238}U	0.001	0.03
^{133}Cs	0.002	0.21			

* Interference with $^{40}Ar^{12}C$ ion. # due to iron oxide.

** Contamination during sample preparation with Pt-Au crucibles.

*** Contamination during sample preparation, because graphite targets were pressed with Tantalum plat.

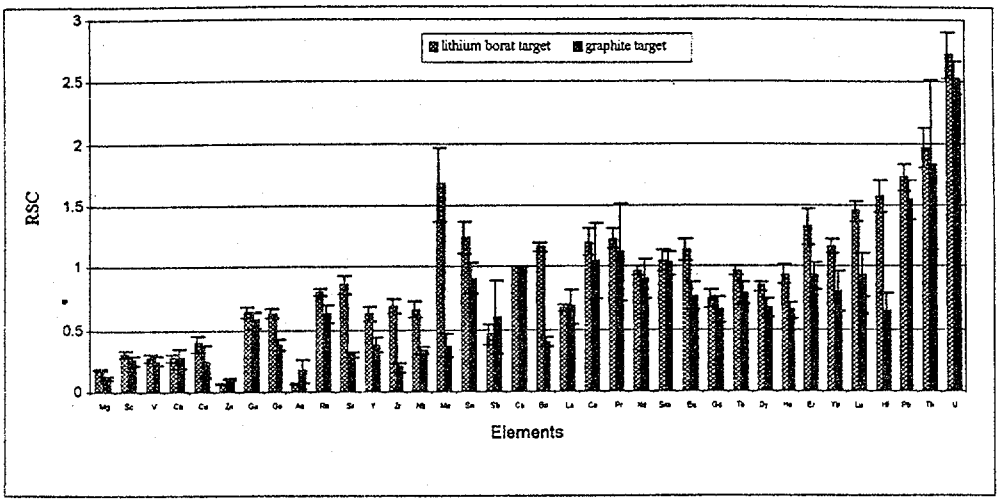

Fig.(3): The relative sensitivity coefficient, RSC (internal standard element; Cesium)

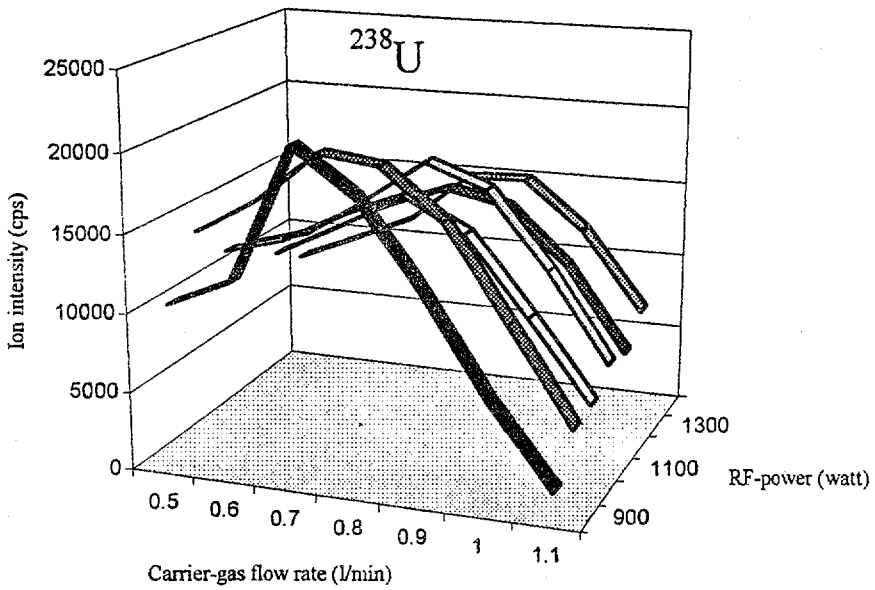

Fig.(4): Ion intensity of Uranium vs sample gas flow rate and RF power

Table(3): Comparison of the determined concentrations by LA-ICP-MS in the granite Sample 1 from Hiroshima (strontium is internal standard).

Element	Reference value		Graphite target	Lithium borate target
	method	(μg/g)	[μg/g]	[μg/g]
Sc	NAA	5.73	5.6 ± 0.43	7.1 ± 0.42
V	DCP	16.3	9.9 ± 0.56	< 19
Cr	ICP	3.5	< 8	< 11
Co	NAA	3.9	5.7 ± 0.24	2.1 ± 0.40
Cu	ICP	5.5	5.6 ± 1.26	< 3.5
Zn	ICP	89.5	129 ± 13	119 ± 2.9
Ga	ICP	22.2	25.4 ± 0.83	23.9 ± 0.61
Ge	ICP	<10	1.6 ± 0.11	1.4 ± 0.25
As	NAA	1	0.75 ± 0.107	< 2
Rb	ICP	86.7	121 ± 6.9	101 ± 4.1
Y	ICP	22.3	14.9 ± 1.07	24.8 ± 0.9
Zr	XRF	216	204 ± 44.5	267 ± 16.6
Nb	XRF	22.3	20.4 ± 1.12	14.0 ± 0.61
Mo	ICP	<1	0.86 ± 0.377	< 1.3
Ag	ICP	0.5	0.2 ± 0.04	-
Sn	XRF	<2.0	< 2.1	2.2 ± 0.39
Sb	NAA	0.2	0.05 ± 0.013	< 0.7
Cs	NAA	2.4	3.4 ± 0.44	3 ± 0.16
Ba	XRF	931	1054 ± 70.2	871 ± 59.2
La	NAA+ICPMS	29.5	12 ± 3.9	37 ± 4.7
Ce	ICPMS	58	21.3 ± 6.02	65 ± 4.9
Pr	ICPMS	6	2.5 ± 0.53	7.6 ± 0.51
Nd	ICPMS	24.9	13.4 ± 2.81	38 ± 2.5
Sm	NAA	4.92	2.74 ± 0.354	6.8 ± 0.46
Eu	ICPMS+NAA	1.43	1.02 ± 0.109	1.8 ± 0.15
Gd	ICPMS	4.8	3.6 ± 0.38	8.1 ± 0.32
Tb	ICPMS+NAA	0.7	0.5 ± 0.05	1.0 ± 0.04
Dy	ICPMS	3.6	3.6 ± 0.37	6.8 ± 0.29
Ho	ICPMS	0.68	0.67 ± 0.062	1.1 ± 0.05
Er	ICPMS	1.7	1.2 ± 0.13	2.0 ± 0.12
Yb	NAA	1.61	1.36 ± 0.136	2.2 ± 0.09
Lu	NAA	0.22	0.16 ± 0.018	0.26 ± 0.022
Hf	NAA	5.69	4.8 ± 1.03	6.7 ± 0.30
Pb	ICP	10.7	21 ± 1.3	25 ± 1.1
Th	NAA	4.4	3.95 ± 0.705	7 ± 0.5
U	NAA	0.95	0.54 ± 0.043	0.52 ± 0.023

Table (4): Comparison of the determined concentrations by LA-ICP-MS in the granite Sample 4 from Hiroshima (strontium is internal standard).

Element	Reference value		Graphite target	Lithium borate target
	method	(μg/g)	(μg/g)	(μg/g)
Sc	NAA	5.73	6.5 ± 0.64	8.3 ± 0.34
V	DCP	16.3	11.4 ± 1.22	< 19
Cr	ICP	3.5	< 8	< 11
Co	NAA	3.9	6.3 ± 0.43	2.6 ± 0.33
Cu	ICP	5.5	5.5 ± 0.57	6.1 ± 2.74
Zn	ICP	89.5	136 ± 13	133 ± 11
Ga	ICP	22.2	27.8 ± 2.92	29.4 ± 3.15
Ge	ICP	<10	1.9 ± 0.14	1.6 ± 0.17
As	NAA	1	0.95 ± 0.118	< 2
Rb	ICP	86.7	137 ± 8.5	105 ± 3.6
Y	ICP	22.3	15.7 ± 1.04	24.9 ± 0.84
Zr	XRF	216	174 ± 43.1	281 ± 12
Nb	XRF	22.3	22.2 ± 1.22	15.2 ± 0.71
Mo	ICP	<1	0.80 ± 0.154	< 1.3
Ag	ICP	0.5	0.3 ± 0.12	-
Sn	XRF	<2.0	< 2.1	2.2 ± 0.46
Sb	NAA	0.2	0.08 ± 0.025	< 0.7
Cs	NAA	2.4	3.9 ± 0.41	3.3 ± 0.16
Ba	XRF	931	1135 ± 30.2	953 ± 27
La	NAA+ICPMS	29.5	14.5 ± 4.59	45 ± 2
Ce	ICPMS	58	25.6 ± 7.04	75 ± 3
Pr	ICPMS	6	3.2 ± 0.61	8.6 ± 0.36
Nd	ICPMS	24.9	15.2 ± 3.93	43 ± 1.5
Sm	NAA	4.92	3.3 ± 0.40	7.8 ± 0.41
Eu	ICPMS+NAA	1.43	1.1 ± 0.09	1.9 ± 0.13
Gd	ICPMS	4.8	3.9 ± 0.33	8.9 ± 0.59
Tb	ICPMS+NAA	0.7	0.5 ± 0.03	1.0 ± 0.05
Dy	ICPMS	3.6	3.9 ± 0.43	7.2 ± 0.50
Ho	ICPMS	0.68	0.69 ± 0.070	1.2 ± 0.03
Er	ICPMS	1.7	1.3 ± 0.13	2.1 ± 0.14
Yb	NAA	1.61	1.41 ± 0.146	2.3 ± 0.18
Lu	NAA	0.22	0.17 ± 0.014	0.25 ± 0.034
Hf	NAA	5.69	4.5 ± 0.67	6.9 ± 0.63
Pb	ICP	10.7	27 ± 6.5	20 ± 0.6
Th	NAA	4.4	5.2 ± 1.75	8.2 ± 0.38
U	NAA	0.95	0.81 ± 0.372	0.83 ± 0.034

purity graphite matrix. Ga, Sn, Tb, Ho, Er, Yb, Lu, Hf and U showed good agreement values in case of lithium-borate fusion and high purity graphite with the reference values. Cs, Pr and Eu also showed good accuracy in lithium-borate fusion. The measured values for Zn, Rb, Cr and Pb showed higher values above the reference values.

Inspection of the measured values in sample 4, shows the same trend and showed an agreement with the measured values as in sample 1. However, no significant differences in data obtained by the two methods of sample preparation and this differences are due to inhomogeneity of sample in case of high purity graphite target and small amount of sample required to prepare target by lithium-borate fusion. Finally, a comparison of the results obtained for Hiroshima samples and that obtained for granite GM standard reference material, it demonstrated that there is no large difference between them. So, it is concluded that the irradiated granite sample form Hiroshima are naturally occurance with a normal trace element concentrations.

Isotope ratio

For the isotope ratio measurements it is necessary to optimize the laser ablation system and the ICP-MS instrument. The most important parameters are the radio frequency power and carrier gas flow rate. It is found that the maxim ion intensity of Uranium appears at 900 Watt RF-power and 0.7 l/min carrier gas flow rate, as shown in Fig. (4).

Table (5): Uranium isotope ratio $^{235}U/^{238}U$ determination in a pressed graphite target from Hiroshima granite samples.

Measurement n	Sample 1		Sample 4	
	$^{235}U/^{238}U$	SD (n=6)	$^{235}U/^{238}U$	SD (n=6)
1	0.0093	0.0022	0.0083	0.0033
2	0.0089	0.0033	0.0071	0.0019
3	0.0094	0.0028	0.0073	0.0019
4	0.0095	0.0030	0.0071	0.0019
5	0.0076	0.0021	0.0076	0.0023
6	0.0081	0.0020	0.0085	0.0023
7	0.0080	0.0027	0.0088	0.0023
8	0.0082	0.0019	0.0078	0.0011
9	0.0076	0.0023	0.0089	0.0025
10	0.0076	0.0028	0.0089	0.0013
11	0.0096	0.0015	0.0091	0.0030
Mean (n=11)	0.0078		0.0075	
SD (n=11)	0.0008		0.0008	
RSD (%)	10.5		10.4	

Uranium has three naturally occurring isotopes ^{234}U (0.06%), ^{235}U (0.72%) and ^{238}U (99.28%). The principle limitations for the precise measurement of U isotope ratios are the large difference in abundance between the natural isotopes and the low

concentrations which often occur. The measured isotope ratios of Uranium ($^{235}U/^{238}U$) of Hiroshima granite sample using high purity graphite target are 0.0078 ± 0.0008 in sample 1 and 0.0075 ± 0.0008 in sample 4. High standard deviation are caused by the inhomogeneity of the sample, as shown in Table (5). Sixty replicate determinations gave a precision of 10.5 % and 10.4 % in case of sample 1 and sample 4, respectively. So, the measured isotope ratios are higher than expected in natural samples are due to possible interferences on $^{235}U^+$ form the ions $^{155}Gd^{40}Ar_2^+$, $^{208}Pb^{27}Al^+$, $^{207}Pb^{16}O^{12}C^+$, $^{205}Tl^{16}O^{14}N^+$ and $^{203}Tl^{16}O_2^+$.

Acknowledgements

Thanks to Prof. Dr. Nolte (Faculty of Physics, Technical University of Munich), for supplying the samples from Hiroshima and for providing the reference values.

REFERENCES

(1) J. Westheide, J.S. Becker, J.A.C. Broekaert, and H.-J. Dietze; European Plasma Winter conference. Cambridge, 8-13 January (1995).
(2) J.S. Becker, U. Breuer, J. Westheide, A.I. Saprykin, H. Holzbrecher, H. Nickel, and H.-J. Dietze; Fresenius J. Anal. Chem. , 355 , 626(1996).
(3) M. Gastel, J.S. Becker, G. Kuppers, H.-J. Dietze; Spectrochim. Acta, B52, 2051(1997).
(4) J.Th.Westheide,J.S. Becker,R. Jäger, H.-J. Dietze and J.A.C. Broekaert, J. Anal. At. Spectr., 11 , 661(1996).
(5) J.S. Becker and H.-J. Dietze, Spectrochimica Acta, 13B , 1475 (1998).
(6) H. Pang, D. Wiederin, R.S. Houk, and E.S. Yeung; Anal. Chem., 63 , 390(1991).
(7) J.S. Becker, G. Seifert, A.I. Saprykin, and H.-J. Dietze; J. Anal. At. Spectr., 11 , 643(1996).